UCRL-JC-133852
PREPRINT

Modifications in the Grain Boundary Character Distribution in FCC Materials Through Thermomechanical Processing

M. Kumar
A.J. Schwartz
W.E. King

This paper was prepared for submittal to the
International Conference on Texture of Materials
Montreal, Canada
August 9-13, 1999

March 1999

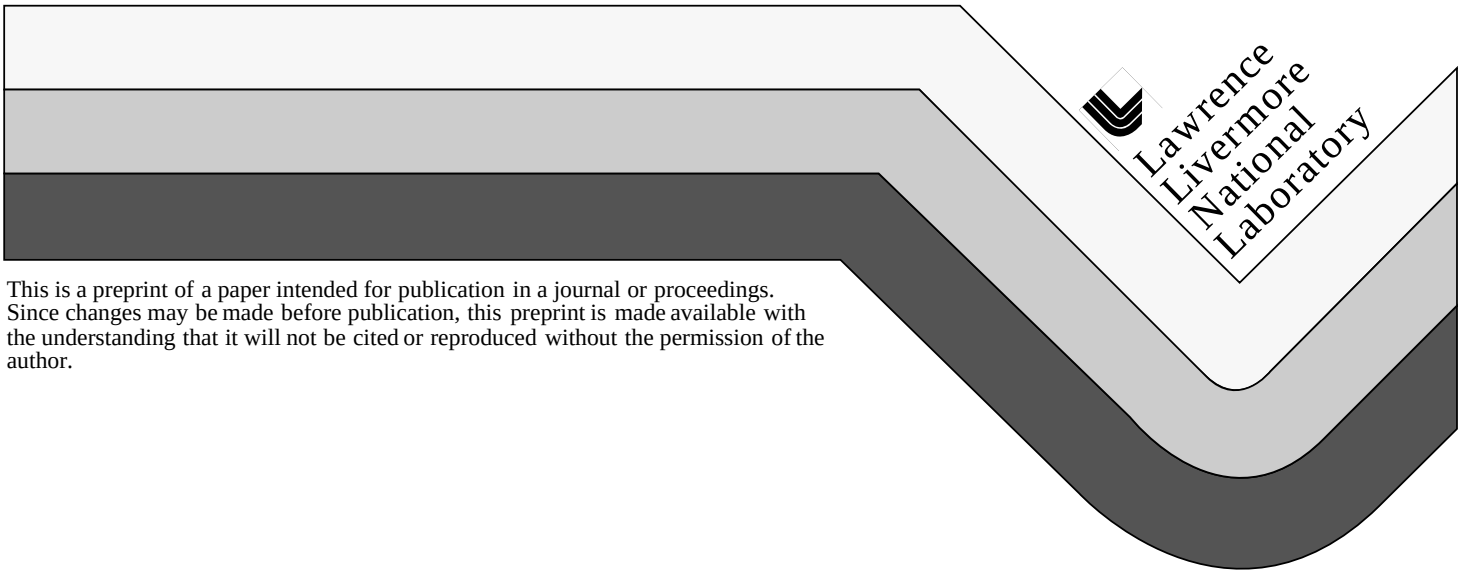

MODIFICATIONS IN THE GRAIN BOUNDARY CHARACTER DISTRIBUTION IN FCC MATERIALS THROUGH THERMOMECHANICAL PROCESSING

M. KUMAR, A.J. SCHWARTZ, and W.E. KING
Lawrence Livermore National Laboratory, Livermore, CA 94550, U.S.A.

ABSTRACT

Recently, a body of work has emerged that indicates the potential to improve certain materials' properties through thermomechanical processing (TMP) solely by controlling grain misorientations. The grain boundary character distribution (GBCD) is defined as a microstructural property that describes the proportions of "special" and "random" boundaries with reference to the coincident site lattice model. Most of the "optimization" treatments reported in the literature have been performed on f.c.c. metals and alloys with medium to low stacking fault energies and have resulted in microstructures with high fractions of $\Sigma 3$, $\Sigma 9$, and $\Sigma 27$ boundaries, or $\Sigma 3^n$ type boundaries. It could be interpreted that only an increased incidence of annealing twinning is required to improve the GBCD. However, it also appears imperative that the formation of annealing twins disrupt the connectivity of the random boundary network, thus implying that $\Sigma 3^n$ reactions and resultant triple junctions are critical. Experiments to modify the GBCD in model materials like oxygen–free electronic Cu and Inconel 600 are presented and the efficacy of the processing routes is assessed in terms of the random boundary network and evolution of texture in the processed microstructures.

Keywords: grain boundary character distribution, special boundaries, annealing twinning, random boundaries

1. INTRODUCTION

Intercrystalline defects, such as grain boundaries and triple lines or junctions, are known to exert influence over several key materials parameters. Therefore the ability to manipulate the population of grain boundary types in the microstructure allows tailoring of properties for specific applications in a manner similar to modifications of the microstructure through solid-state phase transformations.

The concept of "grain boundary design and control" [1] has evolved into "grain boundary engineering." Efforts to engineer grain boundaries have primarily concentrated on changing the misorientation distribution function (MDF) through TMP or through thin film deposition and solidification techniques. The effect is to increase the fraction of grain boundaries in the microstructure that exhibit specific disorientations described by the coincident site lattice (CSL) model [2].

When the appropriate processing conditions are obtained, grain boundary engineering appears to produce materials where the grain size gets refined, the fraction of special boundaries increases, and the deviations from exact CSL misorientations decrease. Despite these changes to the microstructure, there is no significant increase in the observed texture; in fact, the texture strength may actually be reduced.

Two fundamentally different paths have been reported thus far in the literature. One approach has been to strain the material to small to moderate levels on the order of 6-8%, followed by annealing that causes rotations of grain boundaries towards lower energy configurations, *i.e.*, low Σ boundaries [3-6]. This approach, however, requires very lengthy annealing times and leads to considerable grain growth [7,8]. It has been shown, however, that this "fine tuning" approach reduces the deviation, as set by the Brandon criterion [9], of the grain boundaries from the exact CSL disorientation.

The second approach resorts to a multi-cycle treatment of moderate strain levels followed by annealing treatments at relatively high temperatures but for very short times. An important aspect of this approach is the total forming reduction being broken up into several cycles of deformation and recrystallization.

Advances in the engineering of grain boundaries in materials have been facilitated in recent years by the commercialization of Orientation Imaging Microscopy (OIM) [10-12]. This SEM-based technique has superceded other experimental techniques, such as TEM and electron channeling patterns in SEM, for the determination of the GBCD due to the relatively straightforward specimen preparation and the large number of orientation measurements attainable in a relatively short period of time. Thus, advances in engineering of grain boundaries can be ascribed due to the following factors: (1) recognition that grain boundaries play an important role in a number of materials properties, (2) recent evidence that thermomechanical processing can alter the GBCD, and (3) ease of characterization of the GBCD by the OIM technique.

This paper describes the different approaches to the engineering of grain boundaries in low and medium stacking fault energy (SFE) f.c.c. materials that are part of an on-going research program investigating face-centered and body-centered metals and alloys.

2. EXPERIMENTAL METHODOLOGY

Bars of oxygen free electronic (99.99%) Cu and nominal purity Inconel 600 alloy were used for the sequential strain-recrystallization (SR) processing series of experiments described below. Strain-recrystallization refers to the application of moderate levels of deformations (between 20 and 30%) followed by intermediate or high temperature anneals.

Table I. Process sequence for ofe-Cu strain-recrystallization treatments.

	Sample/Process Number		
Process	OFE-AR	SR-N-350	SR-N-400
Strain	As-received	~30%	~30%
Heat Treatment	None	350°C/10 min	400°C/10 min
Grain Size	125 μm	27 μm	35 μm

The ofe-Cu bar, initially in the semi-hard condition, was further deformed 30% in compression. Specimen disks were then annealed in an argon sand bath at temperatures between 350° and 400°C for 10 minutes, as described in Table I.

After water quenching, the specimens were prepared for optical metallography and OIM. This process was repeated for three strain-recrystallization cycles.

The Inconel 600 alloy was chosen in order to examine an alloy with the f.c.c. crystal structure, but with a lower SFE. The series of optimization treatments induced a thickness reduction of 20% per rolling sequence. The bar was annealed at 1000°C for 15 minutes in air followed by water quenching. OIM observations were made after step number 1, 3, 4, and 5 and 7 for a total of six observations including the as-received condition.

Samples were observed in a Hitachi S2700 SEM with an automated OIM attachment (TSL, Inc.) [13]. Typically, OIM scans were carried out in a hexagonal grid using 1.5 to 5 μm step sizes over areas approximately 200×200 to 500×500 μm^2 in dimensions. Plots were produced of confidence index as a function of position and overlaid with boundaries in the range of 2°–15° (low-angle) and 15°–180° (high-angle). The Brandon criterion [9] was applied to identify those boundaries that were special ($1 \leq \Sigma \leq 49$) in nature. The GBCD is reported by number fraction or frequency of occurrence as opposed to the boundary length fraction reported by the TSL, Inc. analysis software. (Note that the Σ1 boundaries were not included in the GBCD for the as-received condition since these materials were in the semi-hard state with a high dislocation density.)

3. RESULTS AND DISCUSSION

The starting material for the strain-recrystallization study was ofe-Cu in the semi-hard condition with a grain size on the order of ~125 μm, but with a few individual grains larger than 500 μm. Therefore, a very high fraction of Σ1 boundaries was observed and hence omitted from the special fraction for better comparison with the processed microstructures. The very low fraction of Σ3 boundaries, as shown in Fig. 1 is rather surprising in light of the low stacking fault energy (~60-70 mJ/m^2) in copper. The first strain-recrystallization treatment provided a large increase in the Σ3 boundaries with a steep drop in the Σ1 boundaries. Fig. 1 demonstrates how the special fraction increases with successive processing using the SR-N-400 strain-recrystallization treatment as an example. The processing successfully increased the number of Σ3 boundaries, the number of $\Sigma 3^n$ boundaries, as well as the total special fraction to approximately 65%.

The 30% compression deformation induced complete recrystallization at 400°C. This was accompanied by a dramatic reduction in the number of Σ1 boundaries in the microstructure. At the same time, the grain size decreased to below 50 μm. Subsequent treatments at this temperature also induced full recrystallization but only insignificant reductions in grain size.

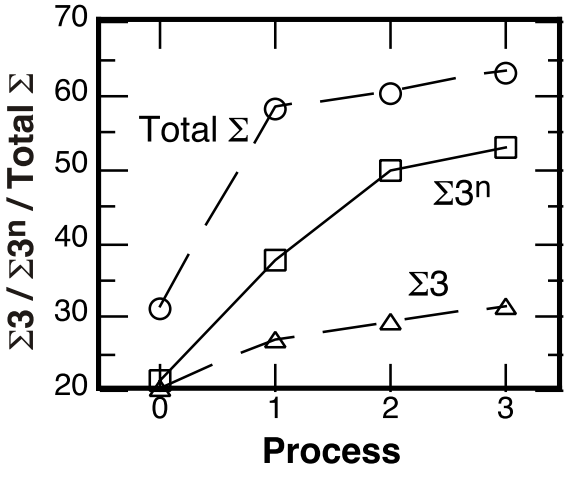

Fig. 1: Distribution of special boundaries with processing sequence in ofe-Cu.

A gradual increase in the fraction of Σ3 boundaries and a dramatic rise in the fraction of Σ9 and Σ27 boundaries was observed, and this can be seen in Fig. 1. The increasing ratio of Σ9 and Σ27 boundaries to twin boundaries is indicative of multiple twinning or twin intersection events, as these $\Sigma 3^n$ boundaries arise from the

geometrical necessity of connecting Σ3 boundaries in the grain boundary network. Pole figures from the as-received and processed ofe-Cu bar are shown in Fig. 2. They indicate a factor of more than two reduction in texture that results from multiple twinning events, as shown by the simulations of Gottstein [14].

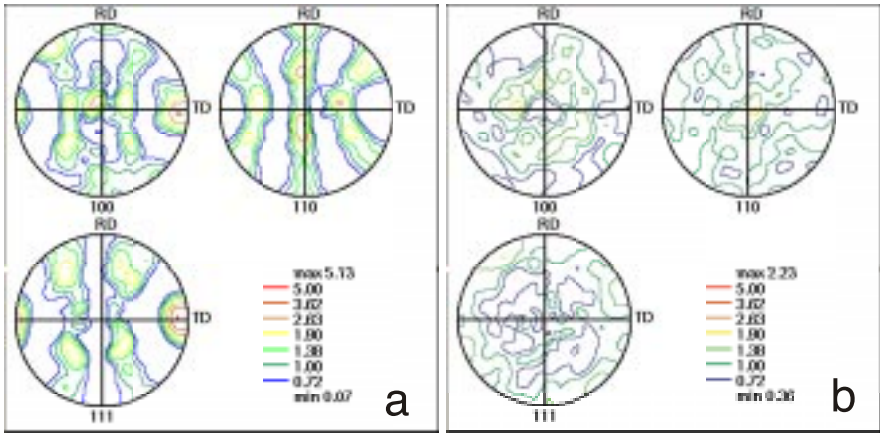

Fig. 2: Pole figures extracted from a) the as-received ofe-Cu bar and b) Cu bar that had been processed to enhance the special fraction, as shown in fig. 1.

The analysis of the Inconel 600 processed samples revealed similar trends (Fig. 3) to those seen for ofe-Cu even though the annealing temperature normalized with respect to the melting temperature was much higher ($0.8T_m$ *vs.* $0.5T_m$ for Cu) in this case. The most notable difference is a slight drop in the fraction of higher order $\Sigma 3^n$ boundaries, even though the fraction of Σ3 boundaries is roughly the same. The reason for this apparent decrease could very well be statistical in nature. The striking point is that in all cases the frequency of Σ3 boundaries levels off at approximately 35-40% of the total number of boundaries, with the ratio of Σ3 boundaries to Σ9 and Σ27 boundaries also peaking at about 3:2. The microstructures do not compare favorably with the ideal twin-limited microstructure [15], as evidenced by the fact that the ratio of Σ3 to other $\Sigma 3^n$ boundaries levels off very early on in the TMP cycle and never approaches the distribution specified by an ideal twin-limited microstructure [15]. The results, however, are in good agreement with the data reported in the literature on GBCD optimization of Ni-base alloys and austenitic stainless steels [16,17].

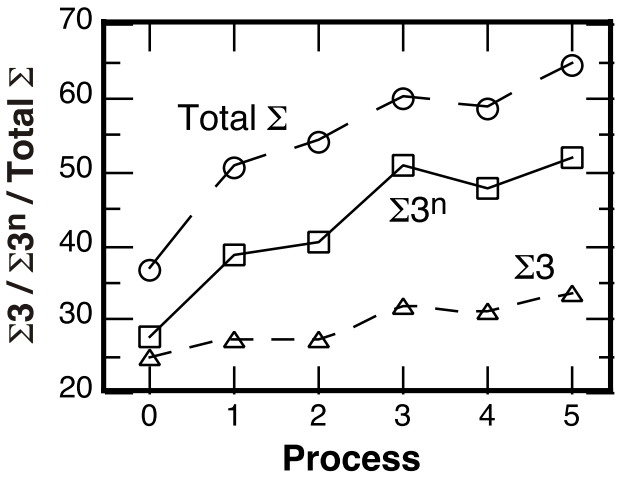

Fig. 3: Distribution of special boundaries with TMP sequence in Inconel 600.

Similar trends were observed [7,8] when the special fractions were

considered in terms of the total length of boundaries rather than by their frequency. However, the fraction of Σ3 boundaries was as high as 50–60% compared with 35–40% when the measurement is by frequency of occurrence. This is a clear indication of a lower energy state being achieved by an increase in the length of low-energy Σ3 boundaries at the expense of relatively higher energy boundaries rather than an increase in their relative fraction of the total number of boundaries in the microstructure. It is interesting to note in this context that the fraction of Σ9 and Σ27 boundaries decreases considerably when measured by length. This concurs with the suggestion [5] that Σ9 and Σ27 boundaries appear in the microstructure as a necessity of geometrical considerations, such as the Σ3 + Σ3 = Σ9 reaction, and not because of a reduction in total energy of the grain boundary network.

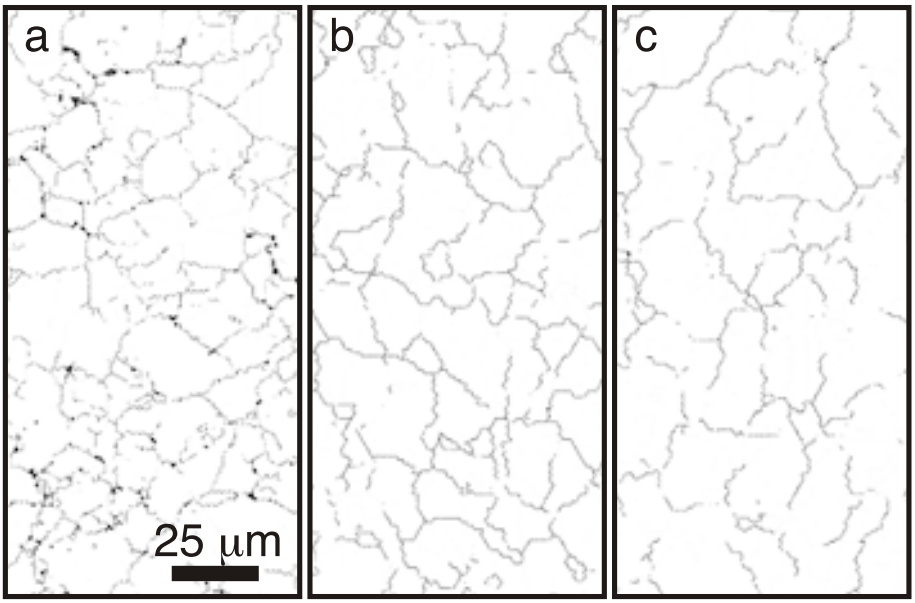

Fig. 4: Reduced OIM scans highlighting only the interconnectivity of random boundaries in the microstructure of Inconel 600 in the following conditions; a) as-received condition, b) after 3 processing cycles, and c) after 5 processing cycles. Note the reduced path length evident after 5 sequential strain and recrystallization cycles.

The idea of grain boundary design has primarily meant the engineering of polycrystalline materials properties through alteration of the GBCD. However, modifications in the GBCD are a necessary, but not sufficient, condition to impact properties such as fracture or corrosion characteristics that are primarily dependent on the spatial distribution and interconnectivity of the boundaries prone to crack propagation. This aspect is qualitatively examined by considering only the random boundaries in the microstructure, as in Fig. 4. From these "reduced" OIM maps it is evident that the network of random boundaries is dramatically altered by the appearance of $\Sigma 3^n$ variant boundaries. Thus there is a strong argument to believe that the continuous path length of undesirable boundaries is severely truncated, as the material is sequentially strain-recrystallized. The problem then remains of finding an appropriate function that describes a critical value for an assembly of random boundaries, and is the subject of on-going investigations.

CONCLUSIONS

It has been demonstrated that the fraction of special boundaries in ofe-Cu and Inconel 600 can be increased through thermomechanical processing. Using commercially practical processing methods, it is possible to increase special fractions to about 70%, while the grain size decreases and no significant texture develops or is randomized. It is shown that the new microstructure is composed of a network of random boundaries interrupted by special boundaries through the process of multiple twinning and formation of $\Sigma 3^n$ variants.

ACKNOWLEDGEMENTS

This work was performed under the auspices of the U.S. Department of Energy and Lawrence Livermore National Laboratory (University of California) under contract no. W-7405-Eng-48. The help of L. Nguyen in the metallographic sample preparation and OIM investigations is gratefully acknowledged.

REFERENCES

1. T. Watanabe, *Res. Mech.*, **11**, p. 47 (1984).
2. H. Grimmer, W. Bollmann, and D. H. Warrington, *Acta Cryst*., **A30**, p. 197 (1974); D. H. Warrington and M. Boon, *Acta Metall*., **23**, p. 599 (1975).
3. L. C. Lim and R. Raj, *Acta Metall*., **32**, p. 117 (1984).
4. V. Randle and A. Brown, *Philos. Mag*., **A59**, p. 1075(1989).
5. C. B. Thomson and V. Randle, *Acta Mater*., **45**, p. 4909 (1997).
6. V. Randle, P. Davies, and B. Hulm, *Philos Mag*., **A79**, p. 305 (1999).
7. W. E. King and A. J. Schwartz, *Mater. Res. Soc. Symp. Proc.*, **458**, p. 53 (1997).
8. W. E. King and A. J. Schwartz, *Scripta Mater*., **38**, p. 449 (1998).
9. D. G. Brandon, *Acta Metall*., **14**, p. 1479 (1966).
10. R. D. Doherty, I. Samajdar, and K. Kunze, *Scripta Metall. Mater*., **27**, p. 1459 (1992).
11. B. L. Adams, *Mater. Sci. Engg*., **A166**, p. 59 (1993).
12. B. L. Adams, S. I. Wright, and K. Kunze, *Metall. Trans.*, **A24**, p. 819 (1993).
13. TSL, Inc. Orientation Imaging Microscopy Software Version 2.5 User Manual (Draper, UT: TSL, Inc. (1997).
14. G. Gottstein, *Acta Metall*., **32**, p. 1117 (1984).
15. G. Palumbo, K. T. Aust, U. Erb, P. J. King, A. M. Brennenstuhl, and P. C. Lichtenberger, *Phys. Stat. Sol*. (a), **131**, p. 425 (1992).
16. P. Lin, G. Palumbo, and K. T. Aust, *Scripta Mater*., **36**, p. 1145 (1997).
17. V. Y. Gertsman and J. A. Szpunar, *Scripta Mater*., **38**, p. 1399 (1998).